



Published in final edited form as:

Gut. 2023 July ; 72(7): 1340–1354. doi:10.1136/gutjnl-2022-327960.

A Pre-clinical Mouse Model of a Misfolded PNLIP Variant Develops Chronic Pancreatitis

Guoying Zhu^{1,2}, Steven J. Wilhelm¹, Leah G. George¹, Brett M. Cassidy¹, Sammy Zino¹, Cliff J. Luke^{1,3}, Mina Hanna¹, Stephen Stone¹, Nhung Phan¹, Neel Matiwala¹, Samuel J. Ballentine⁴, Mark E. Lowe¹, Xunjun Xiao¹

¹Department of Pediatrics, Washington University School of Medicine, St. Louis, Missouri, USA.

²Department of Clinical Nutrition, Putuo People's Hospital, School of Medicine, Tongji University, Shanghai, China.

³Siteman Cancer Center, and Washington University School of Medicine and The Children's Discovery Institute of St. Louis Children's Hospital, St. Louis, Missouri, USA.

⁴Department of Pathology and Immunology, Washington University School of Medicine, St. Louis, Missouri, USA

Abstract

Objective: Increasing evidence implicates mutation-induced protein misfolding and endoplasmic reticulum (ER) stress in the pathophysiology of chronic pancreatitis (CP). The paucity of animal models harboring genetic risk variants has hampered our understanding of how misfolded proteins trigger CP. We previously showed that PNLIP p.T221M, a variant associated with steatorrhea and possibly CP in humans, misfolds and elicits ER stress *in vitro* suggesting proteotoxicity as a potential disease mechanism. Our objective was to create a mouse model to determine if PNLIP p.T221M causes CP and to define the mechanism.

Design: We created a mouse model of *Pnlip* p.T221M and characterized the structural and biochemical changes in the pancreas aged 1-12 months. We used multiple methods including histochemistry, immunostaining, transmission electron microscopy, biochemical assays, immunoblotting, and qPCR.

Results: We demonstrated the hallmarks of human CP in *Pnlip* p.T221M homozygous mice including progressive pancreatic atrophy, acinar cell loss, fibrosis, fatty change, immune cell infiltration, and reduced exocrine function. Heterozygotes also developed CP albeit at a slower rate. Immunoblot showed that pancreatic PNLIP T221M misfolded as insoluble aggregates. The level of aggregates in homozygotes declined with age and was much lower in heterozygotes at all ages. The *Pnlip* p.T221M pancreas had increased ER stress evidenced by dilated ER, increased

Corresponding author: Xunjun Xiao, Ph.D, Department of Pediatrics at Washington University School of Medicine, Campus Box 8208, 660 South Euclid Ave, St Louis, MO 63110, USA, Phone: 314-273-5940; Fax: 314-286-2893; xunjun.xiao@wustl.edu.

Author contribution: Study conceptual design and supervision: MEL, XX

Study experiments, data analysis and interpretation (GZ, SJW, LGG, BMC, SZ, CJL, MH, SS, NP, NM, SJB, MEL, XX)

Manuscript drafting (MEL, XX)

Manuscript revision (GZ, SJW, LGG, BMC, SZ, CJL, MH, SS, NP, NM, SJB, MEL, XX)

Disclosures/conflict of interest statement: The authors disclose no conflicts.

Hspa5 (BiP) mRNA abundance, and a maladaptive unfolded protein response (UPR) leading to up-regulation of *Ddit3* (CHOP), NF- κ B, and cell death.

Conclusion: Expression of PNLIP p.T221M in a pre-clinical mouse model results in CP caused by ER stress and proteotoxicity of misfolded mutant PNLIP.

Keywords

pancreatitis; lipase; protein misfolding; ER stress; cell death

The pancreatic acinar cell is highly specialized in the production, storage, and secretion of large quantities of digestive enzymes¹. To sustain high rates of protein synthesis and maintain endoplasmic reticulum (ER) proteostasis, acinar cells mount a robust response to refold or degrade misfolded proteins². When these adaptive responses fail, overload responses trigger maladaptive inflammatory and cell death pathways, termed proteotoxicity^{3,4}. Proteotoxicity underlies the pathophysiology of over 100 diseases⁵. Multiple observations implicate proteotoxicity in the pathophysiology of chronic pancreatitis (CP), an irreversible, destructive inflammatory disorder of the pancreas⁴. 1) During pancreatitis, pancreatic acinar cells develop dilated ER, a hallmark of pathological ER stress⁶⁻⁸. 2) In experimental models of pancreatitis, ER stress and unfolded protein response (UPR) pathways are activated⁹⁻¹¹. 3) Genetic variants in genes encoding pancreatic enzymes such as *PRSS1*, *CPA1*, *CTRC*, *SPINK1*, and *CEL* result in protein misfolding, increased ER stress, and proteotoxicity in transfected cell culture^{4,12-21}. About 50% of adults and 75% of children with CP have genetic risk variants and most patients suffer from recurrent episodes of acute pancreatitis (RAP) before they develop CP^{22,23}. Thus, discrete episodes of RAP driven by genetic risk factors result in CP. Consequently, restoring proteostasis in the presence of misfolded proteins is an attractive therapeutic strategy to stop RAP and prevent its progression to CP.

At least two critical knowledge gaps have impeded rational development of therapies for CP caused by mutant protein misfolding. First, most misfolding risk variants for CP identified thus far reside within the trypsin network, complicating the interpretation of the underlying pathophysiology. The lack of diverse animal models limits our ability to delineate the role of protein misfolding in genetic risk variants for CP, and to conduct pre-clinical testing of novel therapeutics^{24,25}. Second, we have limited understanding at a molecular level of how accumulation of misfolded protein contributes to disease onset and progression. Therapy development requires detailed understanding of the pathways triggered by misfolded proteins. Hence, there is a pressing need to model CP risk variants in other genes in animals to define the pathogenesis of pancreatitis caused by protein misfolding.

The pancreatic acinar cell produces large quantities of pancreatic triglyceride lipase (PNLIP), which has no known interactions with trypsin. The first report of a genetic variant in *PNLIP* that might cause disease described two brothers with homozygous *PNLIP* p.T221M. The brothers had steatorrhea and evidence of exocrine pancreatic insufficiency (low fecal elastase level) suggesting they have CP²⁶. We previously showed that PNLIP T221M misfolds and elicits ER stress *in vitro* suggesting proteotoxicity as a potential disease mechanism²⁷. Herein, we report a new animal model harboring human *PNLIP*

p.T221M in mouse *Pnlip*^{26 27}. Our aim was to determine if *PNLIP* p.T221M causes CP and, if so, to define the disease mechanism and broaden our understanding of the pathophysiology underlying CP driven by genetic variants causing protein misfolding in highly expressed digestive enzymes.

METHODS

Expression of mouse PNLIP T221M by transient transfection in HEK293T cells was carried out to confirm that mouse PNLIP T221M misfolds and triggers ER stress. A mouse model *Pnlip* p.T221M was generated in C57BL/6N strain using CRISPR/Cas9 technology to change the ACA codon for Thr221 to ATG encoding methionine. Founder animals were identified by deep sequencing and confirmed by dideoxynucleotide sequencing. The first generation of animals from founders were further verified by dideoxynucleotide sequencing and used to expand the colonies. *Pnlip* p.T221M heterozygous animals were bred, and *Pnlip* p.T221M homozygous, heterozygous, and WT mice of both sexes were analyzed from age 1-12 months. The analysis methods included histochemistry, immunohistochemistry, immunofluorescence, transmission electron microscopy (TEM), biochemical assays, protein immunoblot, and quantitative PCR (qPCR). The detailed description of Methods is in the supplementary information.

RESULTS

Creation of the *Pnlip* p.T221M mouse strain

Like human PNLIP T221M, mouse PNLIP T221M expressed in transfected HEK293T had impaired secretion and increased intracellular retention indicative of misfolding, which triggered activation of ER stress as evidenced by elevated levels of intracellular BiP (also known as Grp78 or Hspa5, Fig S1)²⁷. In addition, the mutation abolished the lipase activity of PNLIP (Fig S1). We then introduced the mutation into the *Pnlip* loci of C57BL/6N mice with CRISPR/Cas9 technology and validated the mutation by dideoxynucleotide sequencing (Fig S2). The new mouse strain bred normally. Because the human mutation was described in the homozygous state, we focused on *Pnlip* p.T221M homozygous mice, but also report data on heterozygotes²⁶.

Expression of PNLIP in the pancreas of *Pnlip* p.T221M mice

We next evaluated the trafficking of PNLIP T221M in cultured primary pancreatic acinar cells isolated from *Pnlip* p.T221M homozygous mice at 5 weeks. Relative to WT controls, the secretion of PNLIP T221M into the medium with or without cerulein was significantly decreased when measured by immunoblot or activity assay (Fig S3A-C). The bulk of intracellular PNLIP T221M was in the detergent-insoluble fraction (Fig S3B and C). The decreased secretion of mouse PNLIP T221M and its intracellular retention as detergent-insoluble aggregates is consistent with misfolding of the variant²⁷.

Chronic pancreatitis in the *Pnlip* p.T221M mice

Because CP can affect weight gain, we monitored the body weight of WT and *Pnlip* p.T221M mice over 12 months. The body weight was indistinguishable among the

three genotypes (Fig 1A for males and Fig S4A for females). In contrast, the weights of pancreases isolated from *Pnlip* p.T221M homozygous or heterozygous mice were significantly lighter than those of WT mice; the pancreases of 3 to 12 months-old heterozygotes were intermediate size (Fig 1B for males and Fig S4B for females).

We then used multiple measures to determine if *Pnlip* p.T221M animals develop CP. Consistent with pancreatic acinar cell injury, *Pnlip* p.T221M mice had significantly elevated levels of serum amylase at all ages compared to WT controls (Fig 1C for males and Fig S4C for females). The lower serum amylase activities in homozygotes than heterozygotes may reflect greater loss of exocrine parenchyma. H&E staining of formalin-fixed, paraffin-embedded pancreatic sections showed no discernable changes in WT mice regardless of age; whereas the pancreas from homozygous and heterozygous animals showed loss of acini, infiltration of inflammatory cells, and fatty change that increased with age (Fig 1D for males and Fig S4D for females). Acinar-ductal metaplasia was present but not a prominent feature. The pathology developed slower in heterozygotes. An increase in acinar cell dropout and pancreatic histology score with age further supported the progression of disease in *Pnlip* p.T221M mice (Fig S5).

We demonstrated the presence of fibrosis in the pancreas of 6 month old *Pnlip* p.T221M homozygous mice compared to age-matched WT controls by showing a significant increase in Masson's trichrome staining (Fig 2A and B) and in levels of hydroxyproline content (Fig 2C), in alpha smooth muscle actin abundance (α -SMA) (Fig 2D), and the presence of collagen fibers in the interstitial space by TEM (Fig 2E). A significant increase in α -SMA in the 2 month old *Pnlip* p.T221M pancreas confirmed activation of pancreatic stellate cells shortly after expression of PNLIP begins (Fig 2D).

We next ascertained the presence of inflammation in the pancreas of *Pnlip* p.T221M mice at 3.5 months (Fig 3). Macrophages (F4-80 positive cells) were abundant throughout the pancreas from *Pnlip* p.T221M homozygous mice. CD3+ T cells, B cells, and neutrophils were also present in smaller numbers. These cell types were present in significantly lesser numbers in the WT pancreas. Macrophages were also abundant in the pancreas of heterozygous mice examined at 6 and 12 months (Fig S6).

Because nuclear factor- κ B (NF- κ B) is considered a master mediator of inflammation in pancreatitis, we evaluated if the NF- κ B pathway was up-regulated in the pancreas of *Pnlip* p.T221M homozygous mice by immunoblot and immunohistochemistry of p65, a subunit of NF- κ B complex²⁸⁻³¹. Both p65 and phosphorylated-p65 (p-p65) were significantly increased in the *Pnlip* p.T221M pancreatic extracts than the WT controls by immunoblot (Fig 4A and B). Immunohistochemistry for p65 and p-p65 both showed greater intensity of staining in the *Pnlip* p.T221M pancreas than in WT controls (Fig 4C and D). Furthermore, both p65 and p-p65 showed increased nuclear staining in the *Pnlip* p.T221M pancreas indicative of nuclear translocation of p65³⁰. These data demonstrate up-regulation of the NF- κ B pathway in the pancreas of *Pnlip* p.T221M. Altogether, our findings of pancreatic atrophy, acinar cell loss, fibrosis, fatty change, and inflammation provide strong support for our conclusion that *Pnlip* p.T221M mice spontaneously develop CP.

Reduced pancreatic function in *Pnlip* p.T221M mice

One common complication of CP is impaired exocrine and endocrine pancreatic function. To demonstrate reduced exocrine function in *Pnlip* p.T221M homozygous mice, we documented that *Pnlip* p.T221M homozygous mice had normal fecal fat content when fed regular chow but had steatorrhea when fed a high-fat diet (60% fat calories) (Fig S7). Since our previous work suggests that mouse pancreatic lipase related protein 2 (PNLIPRP2) can compensate for PNLIP deficiency to ensure normal fat assimilation even when fed a high-fat diet, the steatorrhea seen in *Pnlip* p.T221M suggests that PNLIPRP2 levels are also reduced^{32 33}. This hypothesis is supported by our finding that pancreatic lipolytic activity in *Pnlip* p.T221M mice at all age is 5-15% of WT controls (Fig 5A), which was much lower than the activity measured in PNLIP-deficient mice (up to nearly 50% of WT controls)³². Taken together, our data support the conclusion that steatorrhea in *Pnlip* p.T221M mice fed a high-fat diet did not result solely from functional deficiency of PNLIP, but resulted from a combination of PNLIP deficiency and the loss of pancreatic exocrine tissue, which decreases the amount of PNLIPRP2 available for fat digestion. We further assessed exocrine function by measuring amylase activity in pancreatic extracts. When normalized to protein content, the amount of amylase from the *Pnlip* p.T221M pancreas was comparable to WT levels at 1 month, but was significantly decreased at 2, 6, and 12 months (Fig 5B). When expressed as the total activity in the pancreas, amylase activity was significantly less in *Pnlip* p.T221M mice than in control animals at all ages. These findings are consistent with exocrine pancreatic insufficiency.

CP-associated diabetes, also known as type 3c diabetes, has gained attention in recent years³⁴. To assess the endocrine pancreatic function of aged *Pnlip* p.T221M homozygous male mice, we first conducted a glucose tolerance test after overnight fasting for 16 hours. Neither the blood glucose dynamics nor the fasting plasma insulin levels differed between in *Pnlip* p.T221M and WT mice (Fig S8A-C). Next, we closely examined the overall appearance of islets on the H&E stained pancreatic sections. The healthy morphology of islets was preserved in the *Pnlip* p.T221M pancreas when compared to the WT control (Fig S8D). Lastly, we conducted the immunohistochemistry staining of the pancreatic sections for insulin. There was no difference in insulin or glucagon staining between in the *Pnlip* p.T221M mice and WT controls (Fig S8D and E). These data collectively indicate that the endocrine pancreatic function is preserved in *Pnlip* p.T221M mice despite advanced pathological changes in the exocrine pancreas. Further study may be needed to evaluate the endocrine pancreatic function of *Pnlip* p.T221M mice when challenged with high-fat and high-sugar diets or alcohol consumption.

Activation of trypsinogen in the pancreas of *Pnlip* p.T221M mice

To determine if trypsinogen was inappropriately activated to trypsin, we measured trypsin activity in pancreatic extracts. Trypsin activity normalized to protein content was significantly higher in the pancreas of *Pnlip* p.T221M homozygous mice compared to WT mice at 1, 2, and 6 months but not at 12 months, where pancreatic trypsin was significantly higher in WT mice (Fig 5C). When expressed as the total amount of trypsin in the pancreas, the levels were higher in the *Pnlip* p.T221M mice at 1 and 2 months, similar at 6 months, and higher in WT mice at 12 months.

Localization of PNLIP in the pancreas of *Pnlip* p.T221M mice

To identify the cellular location of PNLIP and PNLIP T221M in pancreatic acinar cells, we performed immunofluorescence on mouse pancreatic sections. In the pancreas from WT mice, PNLIP was located in puncta that co-localized with staining for amylase consistent with the presence of PNLIP in zymogen granules (Fig 6A). In contrast, staining for PNLIP T221M was more diffuse and poorly correlated with amylase. When we co-stained pancreatic sections for PNLIP and calreticulin, an ER marker, overlap of the two was minimal in acinar cells from WT mice whereas there was significant overlap in acinar cells from *Pnlip* p.T221M mice (Fig 6B). Taken together, the immunostaining suggests a large fraction of PNLIP T221M was retained in the ER.

Misfolding of PNLIP in the pancreas of *Pnlip* p.T221M mice

To determine if PNLIP T221M misfolds and activates the UPR pathway in the pancreas, we made detergent extracts of the pancreas at various ages and determined if mouse PNLIP T221M formed detergent-insoluble aggregates (Fig 7A). Both PNLIP WT and T221M were present in the detergent-soluble fraction whereas only PNLIP T221M was detectable in the detergent-insoluble fraction (Fig 7A). The amount of aggregated PNLIP T221M decreased with age, whereas the amount in the soluble fraction was consistently similar to WT levels (Fig 7B). The level of detergent-insoluble PNLIP T221M aggregates was much lower in *Pnlip* p.T221M heterozygotes than homozygotes, accounting for less than 1% of total intracellular PNLIP from age 1 through 12 months (Fig S9).

Cell signaling pathways activated in the pancreas of *Pnlip* p.T221M mice

We next provided evidence for increased ER stress in the pancreas from *Pnlip* p.T221M homozygous mice through molecular and imaging approaches. Immunoblots for BiP in detergent-soluble and -insoluble fractions of mouse pancreatic extracts showed that BiP was significantly decreased in the detergent-soluble fraction from *Pnlip* p.T221M mice at all ages examined except for 1 month (Fig 7A and B). In the detergent-insoluble fraction, BiP was only detected in *Pnlip* p.T221M mice suggesting that BiP might be bound to aggregates of misfolded PNLIP T221M³⁵. In contrast to the protein results for BiP, the mRNA levels for *Hsp5a* (BiP) were significantly up-regulated in the pancreas of *Pnlip* p.T221M mice relative to WT animals at all ages after 1 month (Fig 7C). TEM demonstrated that acinar cells from *Pnlip* p.T221M mice at 6 months had dilated ER, a direct indicator of ER stress (Fig 7D). These results are consistent with ER stress caused by misfolding of PNLIP T221M. The size distribution of the zymogen granules skewed toward significantly smaller granules in the *Pnlip* p.T221M acinar cells suggesting decreased production of digestive enzymes as expected with the UPR (Fig S10).

In cells undergoing ER stress, a complex network of cellular signaling pathways, collectively termed as the UPR, can be invoked to restore ER homeostasis^{36 37}. To determine if expression of PNLIP T221M triggered the UPR, we measured the levels of components of each arm of the UPR in the pancreas from WT and *Pnlip* p.T221M homozygous mice (Fig 8). The mRNA levels of X-box binding protein 1 (*Xbp1*) spliced form normalized to total *Xbp1* did not differ between genotypes at any age except for a decrease at 3 months (Fig 8A). The mRNA levels of *Atf6* were upregulated in *Pnlip*

p.T221M mice at all ages but 1 month suggesting this arm of the UPR is activated (Fig 8A). The mRNA levels of two downstream components of the PERK pathway, *Atf4* and *Atf3*, were significantly upregulated at all ages except for 1 month for *Atf4* (Fig 8A). Together, the data support the activation of the PERK arm of the UPR. We also immunoblotted for total eIF2 α and its phosphorylated form, p-eIF2 α . Protein levels of total eIF2 α did not differ between genotypes at any age. The amount of p-eIF2 α was significantly increased in *Pnlip* p.T221M mice at only 3 months but not at the other ages (Fig 8B). The immunohistochemistry of p-eIF2 α showed more tense staining in the *Pnlip* p.T221M pancreatic sections than the WT controls at 3 months (Fig 8C). Lastly, the mRNA levels of DNA damage-inducible transcript 3 (*Ddit3*, also known as CHOP) were significantly increased in the pancreas of *Pnlip* p.T221M animals at all ages (Fig 8D). In sum, these results support the hypothesis that expression of misfolded PNLIP T221M in the pancreas overwhelms the cellular pathways that restore homeostasis during ER stress.

A major consequence of unmitigated ER stress is cell death. Thus, we examined pancreatic sections from *Pnlip* p.T221M homozygous mice for evidence of cell death. H&E staining of pancreatic sections at 3.5 months showed shrunken cells with pyknotic nuclei and cells with pale eosinophilic cytoplasm and cytoplasmic vacuoles indicative of cell death (Fig 9A). In addition, significantly more cells in pancreatic sections from *Pnlip* p.T221M mice were positive for cleaved caspase-3 and for terminal deoxynucleotidyl transferase dUTP nick end labeling (TUNEL) (Fig 9B and C). Furthermore, most nuclei in the pancreas of both genotypes stained positively for high mobility group box 1 (HMGB1). However, cells with little or no nuclear staining and cytoplasmic staining were significantly more abundant in the *Pnlip* p.T221M pancreatic section suggesting translocation of HMGB1 from nucleus to cytoplasm and release into the extracellular space (Fig 9D). These results support the hypothesis that pancreatic expression of misfolded PNLIP T221M triggers a maladaptive cell response leading to cell death and CP.

DISCUSSION

The original report of two brothers homozygous for p.T221M in *PNLIP* did not provide definitive evidence that the mutation causes CP²⁶. To test the hypothesis that *PNLIP* p.T221M causes CP, we generated a knock-in animal model of human *PNLIP* p.T221M in the mouse *Pnlip* loci. *Pnlip* p.T221M mice develop a progressive phenotype of CP including pancreatic atrophy, acinar cell loss, fatty change, fibrosis, infiltration of inflammatory cells, and exocrine pancreatic insufficiency. The pathological changes in the pancreas were already present at 1 month, only 2 weeks after the expression of PNLIP first appears^{38 39}. *Pnlip* p.T221M heterozygous mice exhibit a similar phenotype, albeit the pathology progresses at a slower rate than in the homozygotes. Our model provides the first definitive evidence that genetic variants in *PNLIP* can induce CP.

Genetic variants in *PNLIP* appear to be uncommon in patients with CP, but the incidence of these variants is unknown because genetic studies have rarely included *PNLIP*, and commercial testing is not available for *PNLIP* mutations. One study reported mutations of *PNLIP* in patients with CP⁴⁰. Variants enriched in patients with CP were sensitive to degradation by proteases indicating altered protein structure. Importantly, transfected cells

secreted the protease-sensitive mutants efficiently suggesting that these variants do not cause gross misfolding. Some of the other *PNLIP* variants in subjects and controls were secreted poorly and a subsequent report showed that the mutant proteins misfolded and induced ER stress⁴¹. Direct evidence that these *PNLIP* variants contribute to CP remains lacking.

In cultured cells, proteotoxic protein misfolding drives cellular injury mediated by PNLIP T221M²⁷. Because over-expression of proteins of interest in transfected cells can increase ER stress and complicate the interpretation of these studies, we confirmed that PNLIP T221M caused proteotoxicity in our pre-clinical model. First, we demonstrated misfolded PNLIP T221M aggregates in cultured primary mouse acinar cells and in detergent extracts of pancreas from both homozygous and heterozygous animals. Second, we showed that mutant PNLIP altered its secretory trafficking and had increased retention in the ER. Third, we documented an ER stress response characterized by dilated ER and upregulation of *BiP* mRNA, activation of UPR pathways through increased *Atf6*, *Atf3*, and *Atf4* mRNA and up-regulated p-eIF2 α protein, and ultimately maladaptive pathways downstream of the ER stress response, such as increased *Ddit3* (CHOP) mRNA, up-regulated NF- κ B, increased cell death, and decreased production of zymogens. While other cells such as infiltrating macrophages could contribute to the mRNA measurements, the presence of dilated ER and increased immunostaining for NF- κ B subunit p65 in acinar cells demonstrates maladaptive responses in these cells. Although the mutation of p.T221M inactivates the lipolytic activity of PNLIP, *Pnlip*-deficient mice do not have a CP-like pancreatic phenotype making it unlikely that the lack of PNLIP activity contributes to our findings^{27 32 42}. Taken together, our results implicate proteotoxicity in the pathophysiology of CP in *Pnlip* p.T221M mice, which raises the possibility that misfolded variants in many other acinar cell specific genes might increase risk for CP. Pancreatic acinar cells synthesize large amounts of about 20 digestive enzymes^{43 44}. Because protein synthesis is inherently error-prone, there is a constant flux of destabilized proteins. CP could result when mutations in any of these zymogens increase the mass of unfolded proteins.

Paradoxically, the amount of aggregated PNLIP T221M decreased with age even as the pathological changes in the pancreas progressed. Several explanations for this paradox can be considered. Different populations of acinar cells may express varying levels of zymogens including PNLIP, a concept supported by recent studies of mRNA expression in single cells or nuclei isolated from the pancreas⁴⁵. In this case, cells that express higher levels of PNLIP may be less able to restore homeostasis and die earlier in the course of the disease; whereas acinar cells expressing lower levels of PNLIP may survive longer before succumbing to the continued stress of handling misfolded PNLIP T221M. In our hands, we did observe a small but increased number of acinar cells undergoing cell death in *Pnlip* p.T221M homozygous mice at both 1 and 3 months. Alternatively, there may be ongoing selection for acinar cells that are more efficient in disposing of misfolded proteins, which results in an acinar cell population with gradually decreasing accumulation of misfolded PNLIP in *Pnlip* p.T221M mice. Finally, once the inflammatory response starts, the increased cytokine production and infiltration of inflammatory cells may continue unchecked with ongoing injury and death of acinar cells. To test these hypotheses, future study is warranted to utilize the powerful single-cell (-nuclei) RNA-sequencing to precisely identify cell-specific

transcriptomic signature across different ages to dissect the disease mechanisms in our CP model.

It is of great interest to compare our findings in the *Pnlip* p.T221M model with the findings reported in another model of spontaneous CP related to a human genetic risk variant, *Cpa1* p.N256K²⁴. In contrast to the results reported in this study, the study of the *Cpa1* p.N256K mice found no evidence of dilated ER in acinar cells, did not demonstrate aggregation of CPA1, and had limited evidence for activation of maladaptive pathways. Upregulation of *Hsp5a* (BiP) does not demonstrate proteotoxicity and upregulation of *Ddit3* (CHOP) can occur through pathways unrelated to ER stress or could be present in the infiltrating macrophages²⁴. In a follow-up study, knock-out of *Ddit3* had no effect on pancreatic pathology in *Cpa1* p.N256K mice⁴⁶. Interestingly, intra-pancreatic trypsin activity was elevated in both models, but the levels were higher in the *Cpa1* p.N256K mice than in the *Pnlip* p.T221M mice. The small increase in trypsin activity in the pancreas of *Pnlip* p.T221M mice is likely the by-product of acinar cell injury or death rather than the driving cause for CP. Nevertheless, we cannot rule out the possibility that ER stress somehow triggers trypsin-dependent pathological mechanisms without doing additional investigations⁴⁷. The cellular pathways activated by expression of CPA1 N256K or PNLIP T221M may differ. The clinical phenotypes in humans suggest this may be the case. Heterozygous *CPA1* p.N256K carriers develop early-onset CP with abdominal pain being the main symptom, whereas pain was not a prominent feature in either *PNLIP* p.T221M homozygous or heterozygous carriers^{18 26}. In the preparation of this manuscript, another mouse model of CP through misfolded CEL-HYB1 variant was reported independently by our group and others. The phenotype feature of *Cel-HYB1* mice is the mild focal pathology in the pancreas^{48 49}. Because of these differences, the three models of CP likely will offer complementary insights on the pathophysiology of CP.

In conclusion, we have developed a pre-clinical *Pnlip* p.T221M mouse model that undergoes spontaneous and progressive CP in the presence of misfolded PNLIP T221M, pathological ER stress, and maladaptive cellular responses that trigger inflammatory and cell death pathways. As such, this rare misfolded genetic variant of *PNLIP* can provide important insight into molecular mechanisms common to CP genetic risk variants that are more prevalent. Thus, the *Pnlip* p.T221M mouse will be an invaluable tool to help delineate general underlying mechanisms driving CP through mutation-induced protein misfolding and to uncover novel therapeutic interventions targeted at mitigating proteotoxicity in CP.

Supplementary Material

Refer to Web version on PubMed Central for supplementary material.

Grant support:

This work was supported by The Children's Discovery Institute of Washington University and St. Louis Children's Hospital MI-II-2018-750-2, NIH/NIDDK R01 DK128188 to XX and by NIH/NIDDK R01 DK080820 to MEL. CJL is supported by NIH/NIDDK R01 DK114047 and The Children's Discovery Institute. We gratefully acknowledge Dr. Sanja Sviben and Dr. James Fitzpatrick for their assistance in electron microscopy studies conducted at the Washington University Center for Cellular Imaging (WUCCI), which is supported in part by Washington University School of Medicine, The Children's Discovery Institute (CDI-CORE-2015-505 and CDI-

CORE-2019-813), the Foundation for Barnes-Jewish Hospital (3770) and the Washington University Diabetes Research Center (NIH P30 DK020579). We thank the Genome Engineering and iPSC Center at Washington University School of Medicine in St. Louis for the design and validation of CRISPR/Cas9 reagents and genotyping of mice. We thank the Transgenic, Knockout and Micro-Injection Core and the Mouse Genetics Core at Washington University in St. Louis for mutant mouse production and animal husbandry, respectively.

Abbreviations:

α-SMA	α -smooth muscle actin
ATF	activating transcription factor
BiP	binding immunoglobulin protein, also known as Grp78 or Hspa5
CEL	carboxyl ester lipase
CP	chronic pancreatitis
Ddit3	DNA damage-inducible transcript 3, also known as CHOP
eIF2α	eukaryotic translation initiator factor 2 α
ER	endoplasmic reticulum
HMGB1	high mobility group box 1
IRE1	inositol-requiring protein 1
NF-κB	nuclear factor- κ B
PERK	protein kinase RNA-like ER kinase
PNLIP	pancreatic triglyceride lipase
qPCR	quantitative polymerase chain reaction
UPR	unfolded protein response
RAP	recurrent episodes of acute pancreatitis
TEM	transmission electron microscopy
TUNEL	deoxynucleotidyl transferase-mediated dUTP nick-end labeling
Xbp1	X-box binding protein 1

References

- Whitcomb DC, Lowe ME. Human pancreatic digestive enzymes. *Dig Dis Sci* 2007;52(1):1–17. doi: 10.1007/s10620-006-9589-z [published Online First: 2007/01/06] [PubMed: 17205399]
- Hartl FU. Protein Misfolding Diseases. *Annu Rev Biochem* 2017;86:21–26. doi: 10.1146/annurev-biochem-061516-044518 [published Online First: 2017/04/26] [PubMed: 28441058]
- Pandolfi SJ, Gorelick FS, Lugea A. Environmental and genetic stressors and the unfolded protein response in exocrine pancreatic function - a hypothesis. *Front Physiol* 2011;2:8. doi: 10.3389/fphys.2011.00008 [published Online First: 2011/04/13] [PubMed: 21483727]

4. Sahin-Toth M. Genetic risk in chronic pancreatitis: the misfolding-dependent pathway. *Curr Opin Gastroenterol* 2017;33(5):390–95. doi: 10.1097/MOG.0000000000000380 [published Online First: 2017/06/27] [PubMed: 28650851]
5. O'Reilly LP, Benson JA, Cummings EE, et al. Worming our way to novel drug discovery with the *Caenorhabditis elegans* proteostasis network, stress response and insulin-signaling pathways. *Expert Opin Drug Discov* 2014;9(9):1021–32. doi: 10.1517/17460441.2014.930125 [published Online First: 2014/07/08] [PubMed: 24998976]
6. Churg A, Richter WR. Early changes in the exocrine pancreas of the dog and rat after ligation of the pancreatic duct. A light and electron microscopic study. *Am J Pathol* 1971;63(3):521–46. [published Online First: 1971/06/01] [PubMed: 5581235]
7. Hegewald G, Nikulin A, Gmaz-Nikulin E, et al. Ultrastructural changes of the human pancreas in acute shock. *Pathol Res Pract* 1985;179(6):610–5. doi: 10.1016/S0344-0338(85)80203-X [published Online First: 1985/05/01] [PubMed: 4022838]
8. Lee KT, Ching Sheen P. Effect of gallstones on pancreatic acinar cells. An ultrastructural study. *Eur Surg Res* 1988;20(5-6):341–51. doi: 10.1159/000128784 [published Online First: 1988/01/01] [PubMed: 3224632]
9. Kubisch CH, Logsdon CD. Secretagogues differentially activate endoplasmic reticulum stress responses in pancreatic acinar cells. *Am J Physiol Gastrointest Liver Physiol* 2007;292(6):G1804–12. doi: 10.1152/ajpgi.00078.2007 [published Online First: 2007/04/14] [PubMed: 17431218]
10. Kubisch CH, Logsdon CD. Endoplasmic reticulum stress and the pancreatic acinar cell. *Expert Rev Gastroenterol Hepatol* 2008;2(2):249–60. doi: 10.1586/17474124.2.2.249 [published Online First: 2008/12/17] [PubMed: 19072360]
11. Kubisch CH, Sans MD, Arumugam T, et al. Early activation of endoplasmic reticulum stress is associated with arginine-induced acute pancreatitis. *Am J Physiol Gastrointest Liver Physiol* 2006;291(2):G238–45. doi: 10.1152/ajpgi.00471.2005 [published Online First: 2006/04/01] [PubMed: 16574987]
12. Beer S, Zhou J, Szabo A, et al. Comprehensive functional analysis of chymotrypsin C (CTRC) variants reveals distinct loss-of-function mechanisms associated with pancreatitis risk. *Gut* 2013;62(11):1616–24. doi: 10.1136/gutjnl-2012-303090 [published Online First: 2012/09/04] [PubMed: 22942235]
13. Orekhova A, Geisz A, Sahin-Toth M. Ethanol feeding accelerates pancreatitis progression in CPA1 N256K mutant mice. *Am J Physiol Gastrointest Liver Physiol* 2020;318(4):G694–G704. doi: 10.1152/ajpgi.00007.2020 [published Online First: 20200302] [PubMed: 32116022]
14. Nemeth BC, Orekhova A, Zhang W, et al. Novel p.K374E variant of CPA1 causes misfolding-induced hereditary pancreatitis with autosomal dominant inheritance. *Gut* 2020;69(4):790–92. doi: 10.1136/gutjnl-2019-318751 [published Online First: 20190420] [PubMed: 31005883]
15. Xiao X, Jones G, Sevilla WA, et al. A carboxyl ester lipase (CEL) mutant causes chronic pancreatitis by forming intracellular aggregates that activate apoptosis. *J Biol Chem* 2017;292(19):7744. doi: 10.1074/jbc.A116.734384 [published Online First: 2017/05/14] [PubMed: 28500240]
16. Kereszturi E, Szmola R, Kukor Z, et al. Hereditary pancreatitis caused by mutation-induced misfolding of human cationic trypsinogen: a novel disease mechanism. *Hum Mutat* 2009;30(4):575–82. doi: 10.1002/humu.20853 [published Online First: 2009/02/05] [PubMed: 19191323]
17. Szmola R, Sahin-Toth M. Pancreatitis-associated chymotrypsinogen C (CTRC) mutant elicits endoplasmic reticulum stress in pancreatic acinar cells. *Gut* 2010;59(3):365–72. doi: 10.1136/gut.2009.198903 [published Online First: 2009/12/03] [PubMed: 19951900]
18. Witt H, Beer S, Rosendahl J, et al. Variants in CPA1 are strongly associated with early onset chronic pancreatitis. *Nature genetics* 2013 doi: 10.1038/ng.2730
19. Fjeld K, Weiss FU, Lasher D, et al. A recombinant allele of the lipase gene CEL and its pseudogene CELP confers susceptibility to chronic pancreatitis. *Nature genetics* 2015;47(5):518–22. doi: 10.1038/ng.3249 [published Online First: 2015/03/17] [PubMed: 25774637]
20. Johansson BB, Torsvik J, Bjorkhaug L, et al. Diabetes and pancreatic exocrine dysfunction due to mutations in the carboxyl ester lipase gene-maturity onset diabetes of the young (CEL-MODY): a

- protein misfolding disease. *J Biol Chem* 2011;286(40):34593–605. doi: 10.1074/jbc.M111.222679 [published Online First: 2011/07/26] [PubMed: 21784842]
21. Xiao X, Jones G, Sevilla WA, et al. A Carboxyl Ester Lipase (CEL) Mutant Causes Chronic Pancreatitis by Forming Intracellular Aggregates That Activate Apoptosis. *J Biol Chem* 2016;291(44):23224–36. doi: 10.1074/jbc.M116.734384 [published Online First: 20160920] [PubMed: 27650499]
 22. Kumar S, Ooi CY, Werlin S, et al. Risk Factors Associated With Pediatric Acute Recurrent and Chronic Pancreatitis: Lessons From INSPPIRE. *JAMA Pediatr* 2016;170(6):562–9. doi: 10.1001/jamapediatrics.2015.4955 [published Online First: 2016/04/12] [PubMed: 27064572]
 23. Yadav D, O'Connell M, Papachristou GI. Natural history following the first attack of acute pancreatitis. *Am J Gastroenterol* 2012;107(7):1096–103. doi: 10.1038/ajg.2012.126 [published Online First: 2012/05/23] [PubMed: 22613906]
 24. Hegyi E, Sahin-Toth M. Human CPA1 mutation causes digestive enzyme misfolding and chronic pancreatitis in mice. *Gut* 2019;68(2):301–12. doi: 10.1136/gutjnl-2018-315994 [published Online First: 2018/07/27] [PubMed: 30045879]
 25. Klauss S, Schorn S, Teller S, et al. Genetically induced vs. classical animal models of chronic pancreatitis: a critical comparison. *FASEB J* 2018:fj201800241RR. doi: 10.1096/fj.201800241RR [published Online First: 2018/06/05]
 26. Behar DM, Basel-Vanagaite L, Glaser F, et al. Identification of a novel mutation in the PNLIP gene in two brothers with congenital pancreatic lipase deficiency. *Journal of lipid research* 2014;55(2):307–12. doi: 10.1194/jlr.P041103 [published Online First: 2013/11/23] [PubMed: 24262094]
 27. Szabo A, Xiao X, Haughney M, et al. A novel mutation in PNLIP causes pancreatic triglyceride lipase deficiency through protein misfolding. *Biochimica et biophysica acta* 2015;1852(7):1372–9. doi: 10.1016/j.bbadis.2015.04.002 [published Online First: 2015/04/12] [PubMed: 25862608]
 28. Watanabe T, Kudo M, Strober W. Immunopathogenesis of pancreatitis. *Mucosal Immunol* 2017;10(2):283–98. doi: 10.1038/mi.2016.101 [published Online First: 2016/11/17] [PubMed: 27848953]
 29. Jakkampudi A, Jangala R, Reddy BR, et al. NF-kappaB in acute pancreatitis: Mechanisms and therapeutic potential. *Pancreatology* 2016;16(4):477–88. doi: 10.1016/j.pan.2016.05.001 [published Online First: 2016/06/11] [PubMed: 27282980]
 30. Huang H, Liu Y, Daniluk J, et al. Activation of nuclear factor-kappaB in acinar cells increases the severity of pancreatitis in mice. *Gastroenterology* 2013;144(1):202–10. doi: 10.1053/j.gastro.2012.09.059 [published Online First: 2012/10/09] [PubMed: 23041324]
 31. Rakoncay Z Jr., Hegyi P, Takacs T, et al. The role of NF-kappaB activation in the pathogenesis of acute pancreatitis. *Gut* 2008;57(2):259–67. doi: 10.1136/gut.2007.124115 [published Online First: 2007/08/07] [PubMed: 17675325]
 32. Huggins KW, Camarota LM, Howles PN, et al. Pancreatic triglyceride lipase deficiency minimally affects dietary fat absorption but dramatically decreases dietary cholesterol absorption in mice. *J Biol Chem* 2003;278(44):42899–905. doi: 10.1074/jbc.M303422200 [published Online First: 20030812] [PubMed: 12915407]
 33. Xiao X, Ross LE, Miller RA, et al. Kinetic properties of mouse pancreatic lipase-related protein-2 suggest the mouse may not model human fat digestion. *Journal of lipid research* 2011;52(5):982–90. doi: 10.1194/jlr.M014290 [published Online First: 2011/03/09] [PubMed: 21382969]
 34. Hart PA, Bellin MD, Andersen DK, et al. Type 3c (pancreatogenic) diabetes mellitus secondary to chronic pancreatitis and pancreatic cancer. *Lancet Gastroenterol Hepatol* 2016;1(3):226–37. doi: 10.1016/S2468-1253(16)30106-6 [published Online First: 20161012] [PubMed: 28404095]
 35. Ichhaporia VP, Kim J, Kavdia K, et al. SIL1, the endoplasmic-reticulum-localized BiP co-chaperone, plays a crucial role in maintaining skeletal muscle proteostasis and physiology. *Dis Model Mech* 2018;11(5) doi: 10.1242/dmm.033043 [published Online First: 20180510]
 36. Bhattarai KR, Chaudhary M, Kim HR, et al. Endoplasmic Reticulum (ER) Stress Response Failure in Diseases. *Trends Cell Biol* 2020;30(9):672–75. doi: 10.1016/j.tcb.2020.05.004 [published Online First: 2020/06/21] [PubMed: 32561138]

37. Hetz C. The unfolded protein response: controlling cell fate decisions under ER stress and beyond. *Nat Rev Mol Cell Biol* 2012;13(2):89–102. doi: 10.1038/nrm3270 [published Online First: 2012/01/19] [PubMed: 22251901]
38. Lowe ME, Kaplan MH, Jackson-Grusby L, et al. Decreased neonatal dietary fat absorption and T cell cytotoxicity in pancreatic lipase-related protein 2-deficient mice. *J Biol Chem* 1998;273(47):31215–21. doi: 10.1074/jbc.273.47.31215 [published Online First: 1998/11/13] [PubMed: 9813028]
39. Payne RM, Sims HF, Jennens ML, et al. Rat pancreatic lipase and two related proteins: enzymatic properties and mRNA expression during development. *The American journal of physiology* 1994;266(5 Pt 1):G914–21. doi: 10.1152/ajpgi.1994.266.5.G914 [published Online First: 1994/05/01] [PubMed: 8203536]
40. Lasher D, Szabo A, Masamune A, et al. Protease-Sensitive Pancreatic Lipase Variants Are Associated With Early Onset Chronic Pancreatitis. *Am J Gastroenterol* 2019;114(6):974–83. doi: 10.14309/ajg.0000000000000051 [published Online First: 2019/02/23] [PubMed: 30789418]
41. Toldi V, Kassay N, Szabo A. Missense PNLIP mutations impeding pancreatic lipase secretion cause protein misfolding and endoplasmic reticulum stress. *Pancreatology* 2021;21(7):1317–25. doi: 10.1016/j.pan.2021.07.008 [published Online First: 20210804] [PubMed: 34373204]
42. de Oliveira C, Khatua B, Noel P, et al. Pancreatic triglyceride lipase mediates lipotoxic systemic inflammation. *J Clin Invest* 2020;130(4):1931–47. doi: 10.1172/JCI132767 [PubMed: 31917686]
43. Logsdon CD, Ji B. The role of protein synthesis and digestive enzymes in acinar cell injury. *Nature reviews Gastroenterology & hepatology* 2013;10(6):362–70. doi: 10.1038/nrgastro.2013.36 [published Online First: 2013/03/20] [PubMed: 23507798]
44. Hetz C, Papa FR. The Unfolded Protein Response and Cell Fate Control. *Mol Cell* 2018;69(2):169–81. doi: 10.1016/j.molcel.2017.06.017 [published Online First: 2017/11/07] [PubMed: 29107536]
45. Tosti L, Hang Y, Debnath O, et al. Single-Nucleus and In Situ RNA-Sequencing Reveal Cell Topographies in the Human Pancreas. *Gastroenterology* 2021;160(4):1330–44 e11. doi: 10.1053/j.gastro.2020.11.010 [published Online First: 2020/11/20] [PubMed: 33212097]
46. Nemeth BC, Demcsak A, Geisz A, et al. Misfolding-induced chronic pancreatitis in CPA1 N256K mutant mice is unaffected by global deletion of Ddit3/Chop. *Sci Rep* 2022;12(1):6357. doi: 10.1038/s41598-022-09595-x [published Online First: 20220415] [PubMed: 35428786]
47. Gui F, Zhang Y, Wan J, et al. Trypsin activity governs increased susceptibility to pancreatitis in mice expressing human PRSS1R122H. *J Clin Invest* 2020;130(1):189–202. doi: 10.1172/JCI130172 [published Online First: 2019/09/25] [PubMed: 31550238]
48. Mao XT, Zou WB, Cao Y, et al. The CEL-HYB1 Hybrid Allele Promotes Digestive Enzyme Misfolding and Pancreatitis in Mice. *Cell Mol Gastroenterol Hepatol* 2022 doi: 10.1016/j.jcmgh.2022.03.013 [published Online First: 20220407]
49. Fjeld K, Gravdal A, Brekke RS, et al. The genetic risk factor CEL-HYB1 causes proteotoxicity and chronic pancreatitis in mice. *Pancreatology* 2022;22(8):1099–111. doi: 10.1016/j.pan.2022.11.003 [published Online First: 20221109] [PubMed: 36379850]

What is already known on this topic:

Emerging research suggests proteotoxicity caused by pancreatic misfolded mutant proteins may be another major pathophysiology for chronic pancreatitis besides the trypsin-dependent pathway. Animal models are lacking to dissect molecular mechanisms for this subset of chronic pancreatitis.

What are the new findings:

We demonstrated that the first mouse model harboring a genetic variant in *PNLIP* develops spontaneous and progressive chronic pancreatitis.

We provided the most comprehensive evidence thus far supporting that our new mice develop chronic pancreatitis through cellular pathways activated by mutant protein misfolding.

We showed that the level of misfolded mutant PNLIP aggregate in the pancreas decreases as the disease progresses with age in our model.

How this study might affect research, practice or policy:

This study reports a new pre-clinical model of chronic pancreatitis driven by a variant in a gene that is not part of the trypsinogen-trypsin pathways already known to increase risk for chronic pancreatitis. The model provides a tool to systematically dissect the general role of protein misfolding in chronic pancreatitis and to test novel therapies.

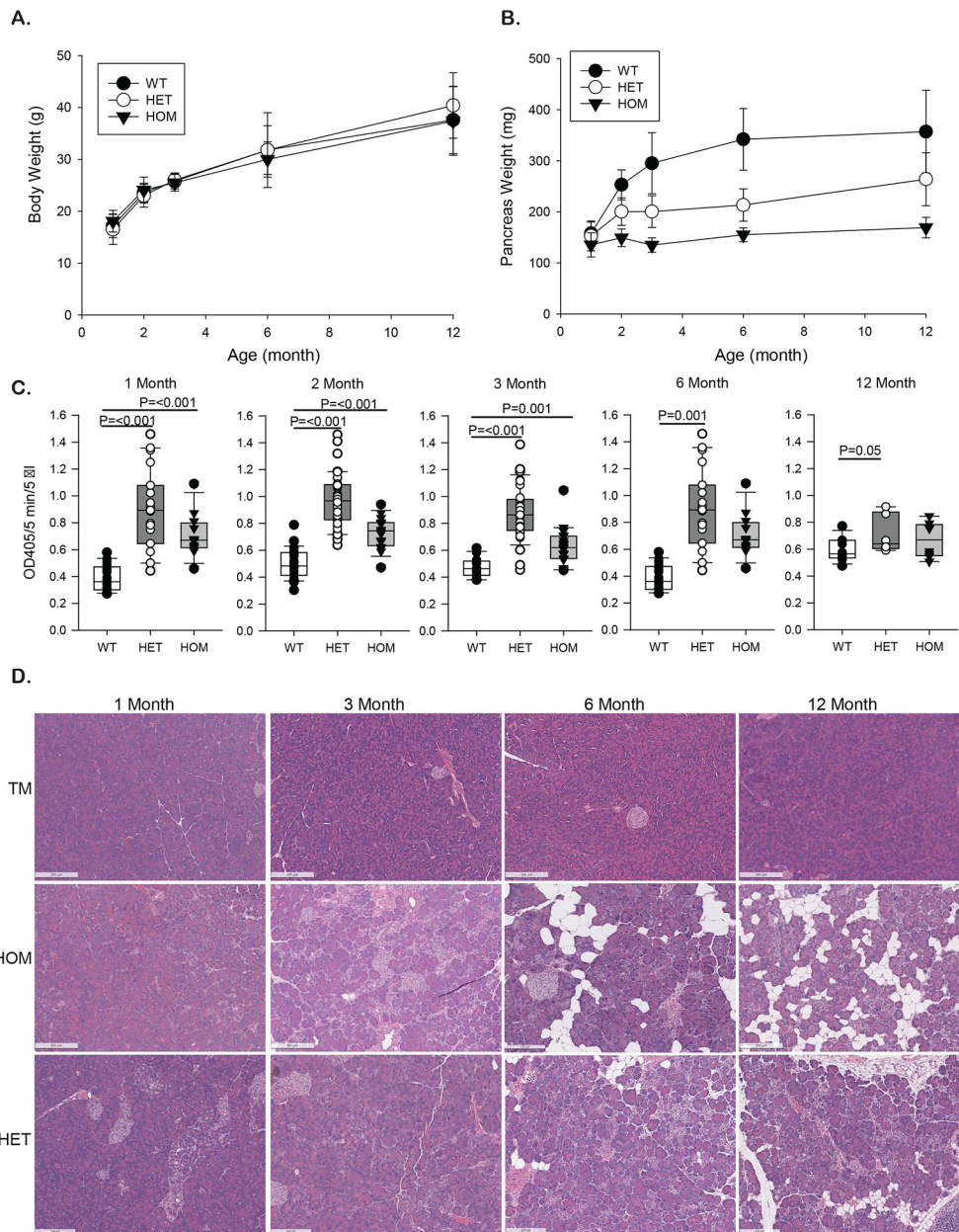


Fig 1. The changes of the pancreas from *Pnlip* p.T221M homozygous (HOM), heterozygous (HET), and wild type (WT) male mice with age from 1-12 months. The quantification graphs are shown as means of individual values with standard deviation at each indicated age. **A.** Body weight. **B.** Pancreas weight. By 2-way ANOVA, there was a statistically significant interaction between genotype and age ($p < 0.001$). The pancreas from both HET and HOM mice was smaller compared to the pancreas from WT mice at all ages except for 1 month ($p < 0.001$). The pancreas from HOM mice were statistically smaller compared to the pancreas from HET mice at all ages except 1 month ($p < 0.001$). **C.** Serum amylase. Multiple t-tests were conducted to compare serum amylase in HOM vs WT mice and HET

mice vs WT mice at each matched age. **D.** H&E stained mouse pancreatic sections. $n > 10$ per genotype at each age point except for $n = 5$ in *D*.

Author Manuscript

Author Manuscript

Author Manuscript

Author Manuscript

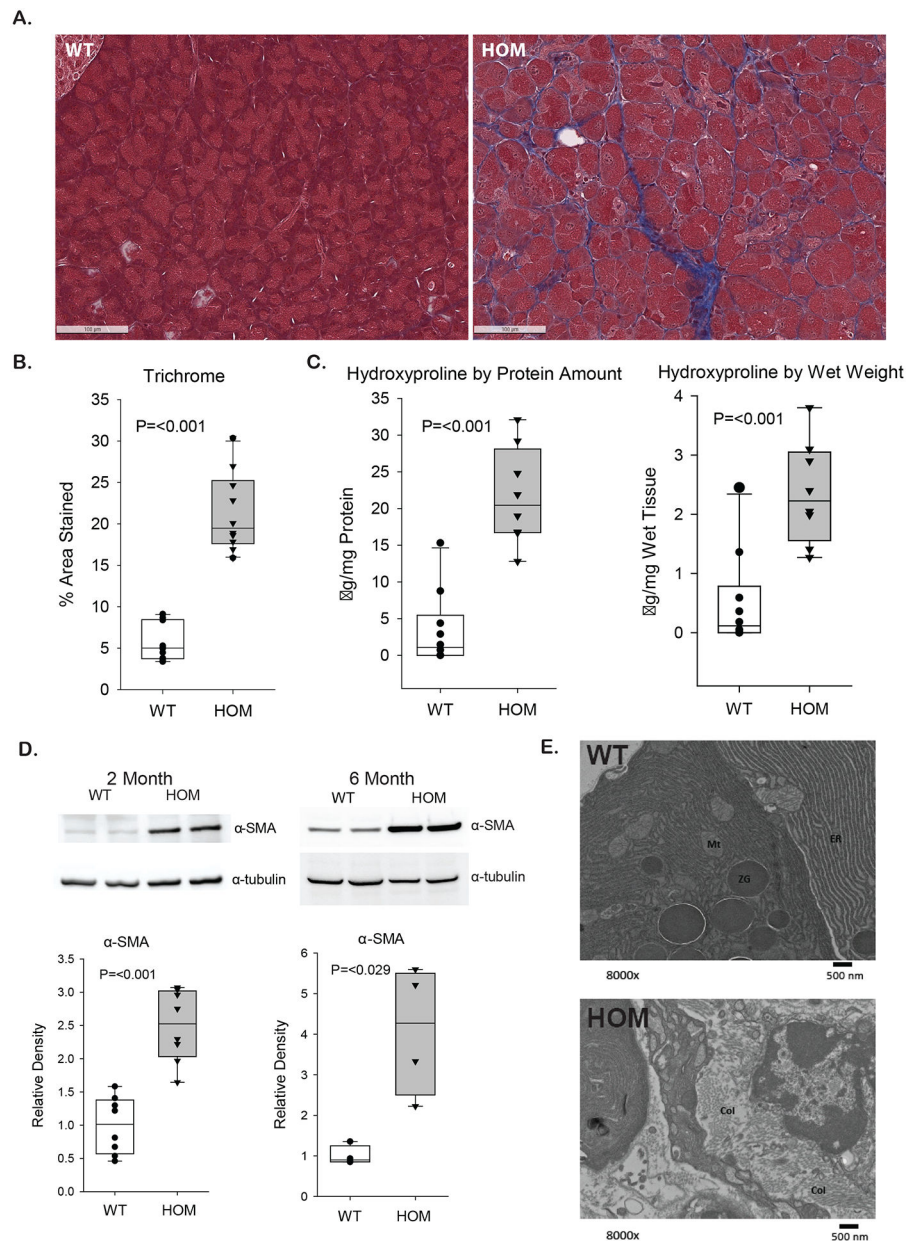


Fig 2. Fibrogenesis in the pancreas from *Pnlip* p.T221M homozygous (HOM) and wild type (WT) mice at age 6 months. **A.** Masson's trichrome staining shows widespread fibrotic change (blue stain) in the pancreas from HOM mice. **B.** The quantification of fibrosis as assessed by trichrome staining shown in **A.** **C.** Hydroxyproline content is increased in the pancreas from HOM mice. **D.** Representative of immunoblots of soluble protein extraction from the mouse pancreas at ages of 2 and 6 months against α -smooth muscle actin (α -SMA), and α -tubulin served as an endogenous control (top panel). The quantification graph of immunoblots (bottom panel). **E.** Transmission electron micrograph (TEM) of the pancreatic sections from HOM mice shows increased collagen (Col), with ER, Mt, and ZG labeled for endoplasmic

reticulum, mitochondria, and zymogen granules, respectively. $n = 3$ in *A*, *B*, and *E*; $n = 6$ in *C*; $n = 4$ in *D*.

Author Manuscript

Author Manuscript

Author Manuscript

Author Manuscript

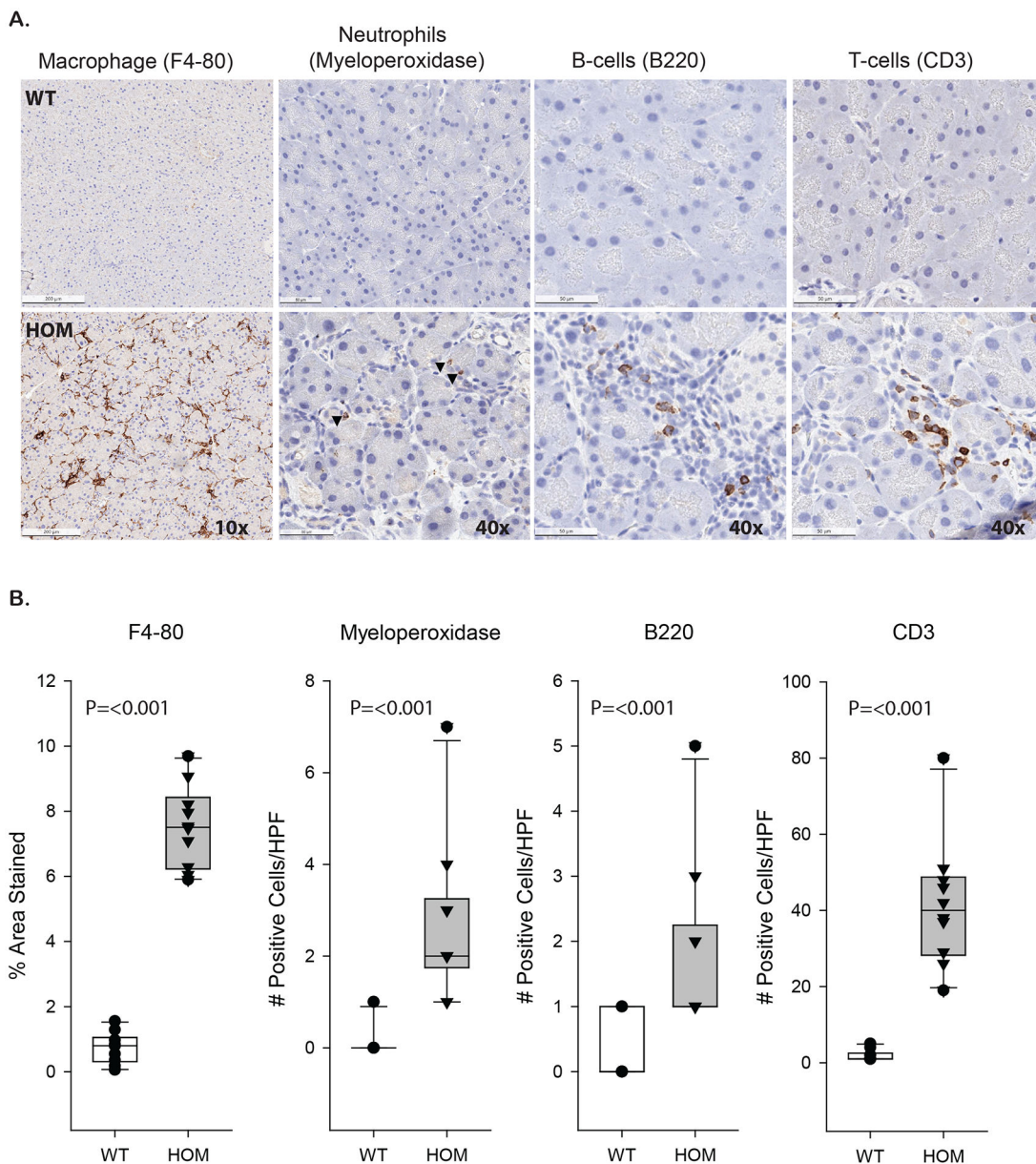


Fig 3. Inflammation in the pancreas of *Pnlip* p.T221M homozygous (HOM) and wild type (WT) mice at age 3.5 months. **A.** Immunohistochemistry stained pancreatic sections from HOM mice show increased immune cell infiltration (brown stain). F4-80 for macrophages, myeloperoxidase for neutrophils, B220/CD45R for B cells, and CD3 for T cells. **B.** The quantification of cells stained positive for each marker shown in **A.** n = 10.

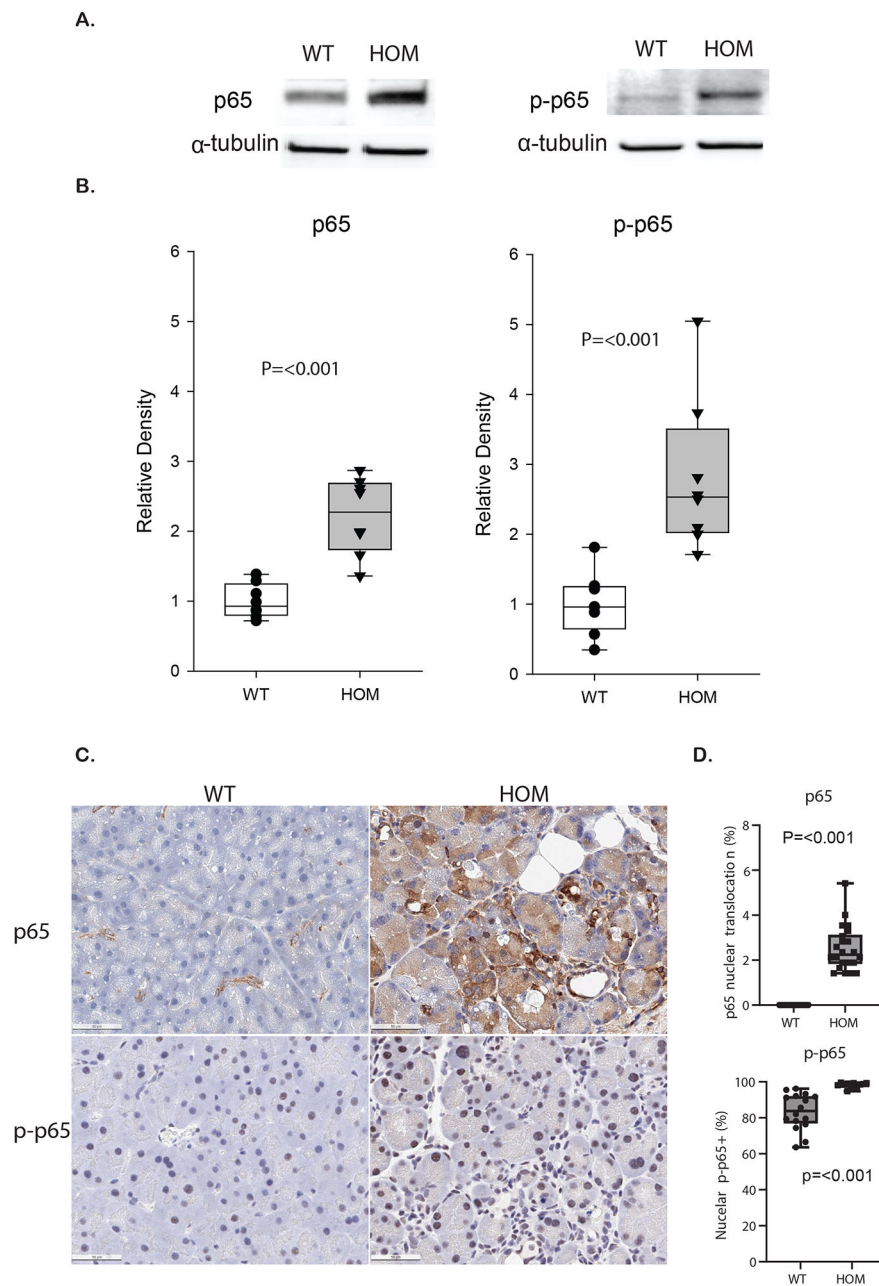


Fig 4. Activation of NF- κ B pathway in the pancreas of *Pn1p* p.T221M homozygous (HOM) and wild type (WT) mice at age 3 months. **A.** Representative immunoblot image for NF- κ B subunit p65 and its phosphorylated form, p-p65, in the soluble pancreatic protein extracts, with α -tubulin serving as an endogenous control. **B.** The quantification graph for the protein abundance of p65 and p-p65 shown in **A.** **C.** Representative image of immunohistochemistry of mouse pancreatic sections for p65 and p-p65. **D.** The quantification of nuclear positive stains for p65 and p-p65. n = 10 for **A** and **B**, and n = 14 for **C** and **D**.

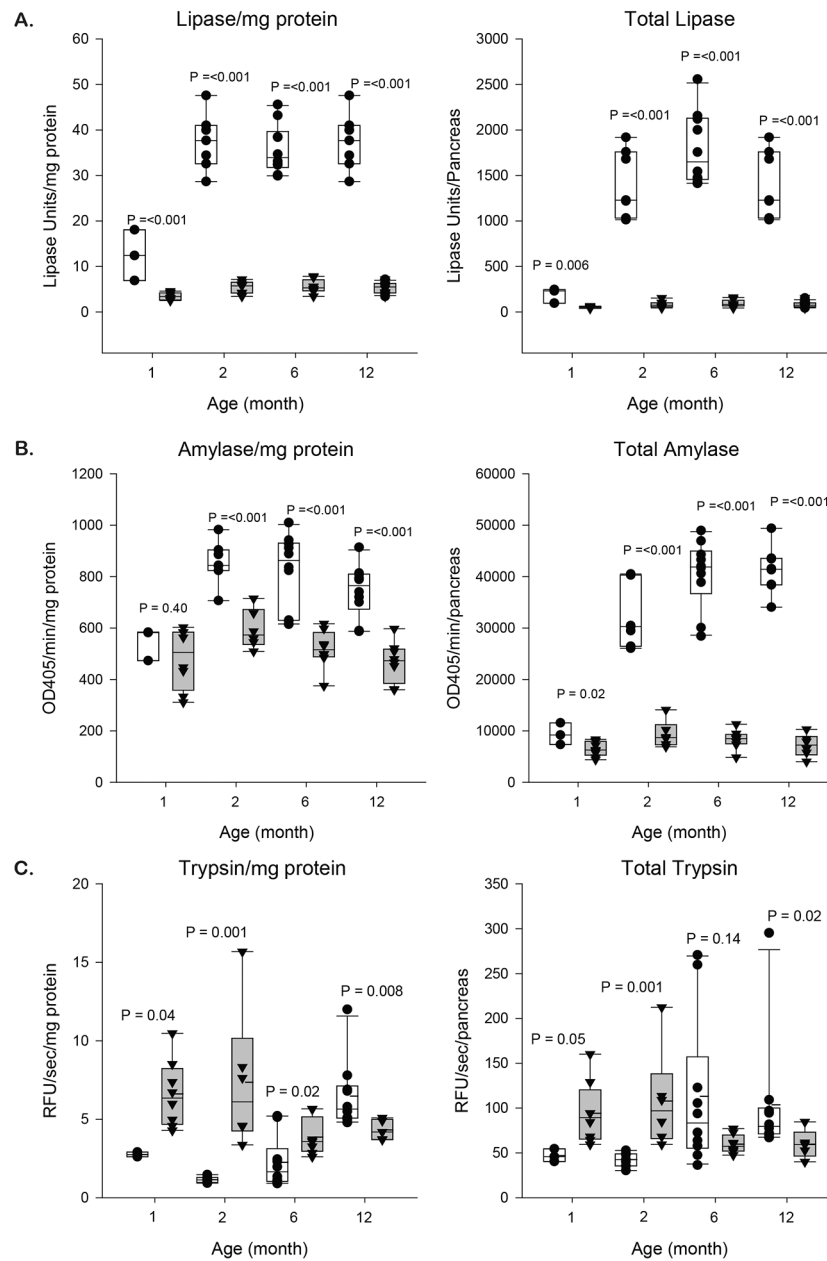


Fig 5. Pancreatic zymogen content from *Pnlip* p.T221M homozygous (HOM) and wild type (WT) mice with age from 1-12 months. **A.** The activity of pancreatic lipase. **B.** The activity of amylase. **C.** The activity of trypsin. The activity of each enzyme was normalized by protein content. Pancreatic total activity for each enzyme was calculated for the entire pancreas. The data are shown as Whiskers plots with individual values and the median box for the 25th to 75th percentiles. $n = 3$ per genotype per age point.

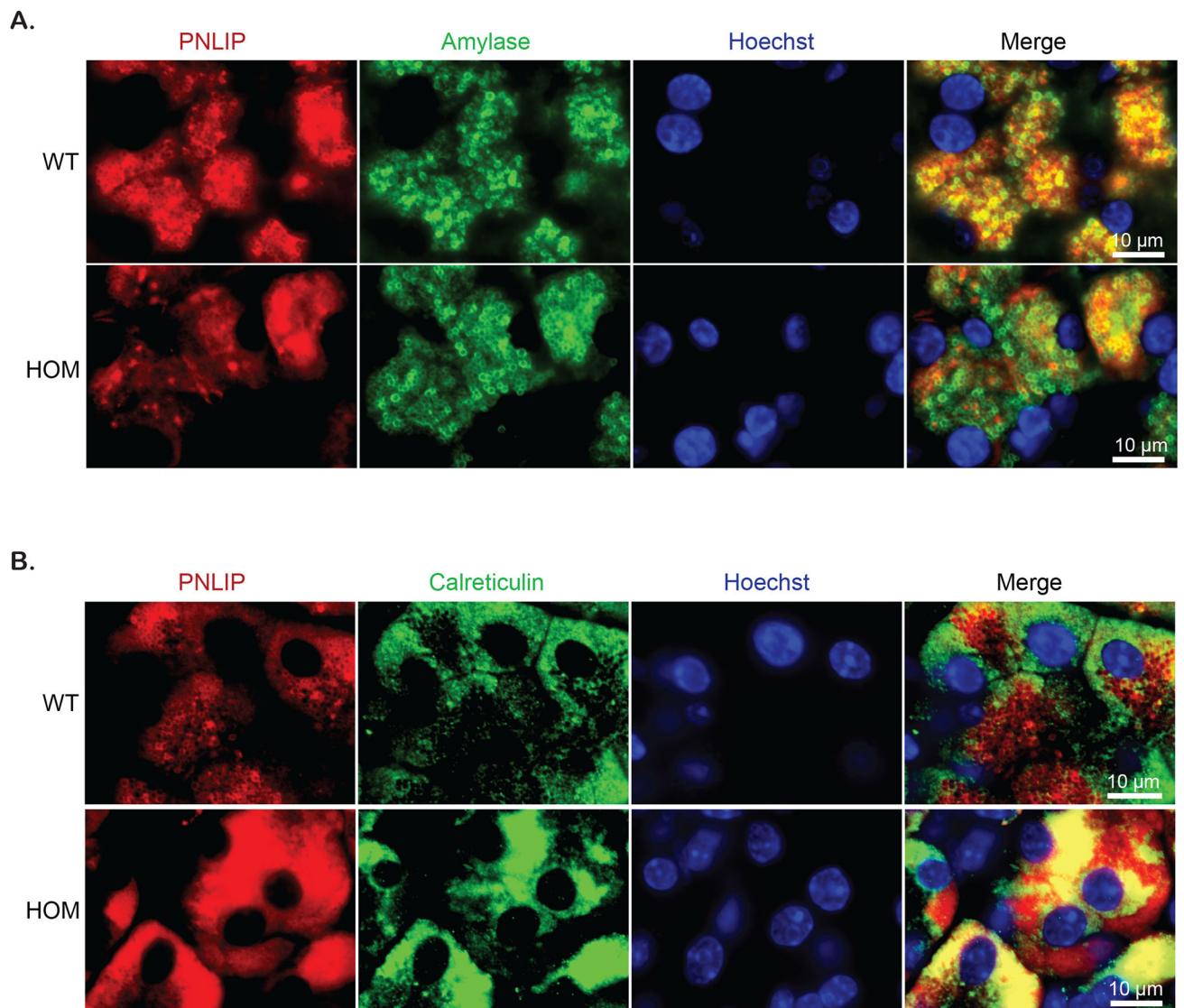


Fig 6. PNLIP trafficking and localization in the pancreatic acinar cells from *Pnlip* p.T221M homozygous (HOM) and wild type (WT) mice at 3 months. Co-immunofluorescence staining was performed on pancreatic sections, and Hoechst stained for nuclear. **A.** Co-immunostaining of PNLIP and amylase (another digestive enzyme); **B.** Co-immunostaining of PNLIP and calreticulin (an ER marker). Bar, 10 μ m. n = 3 per genotype.

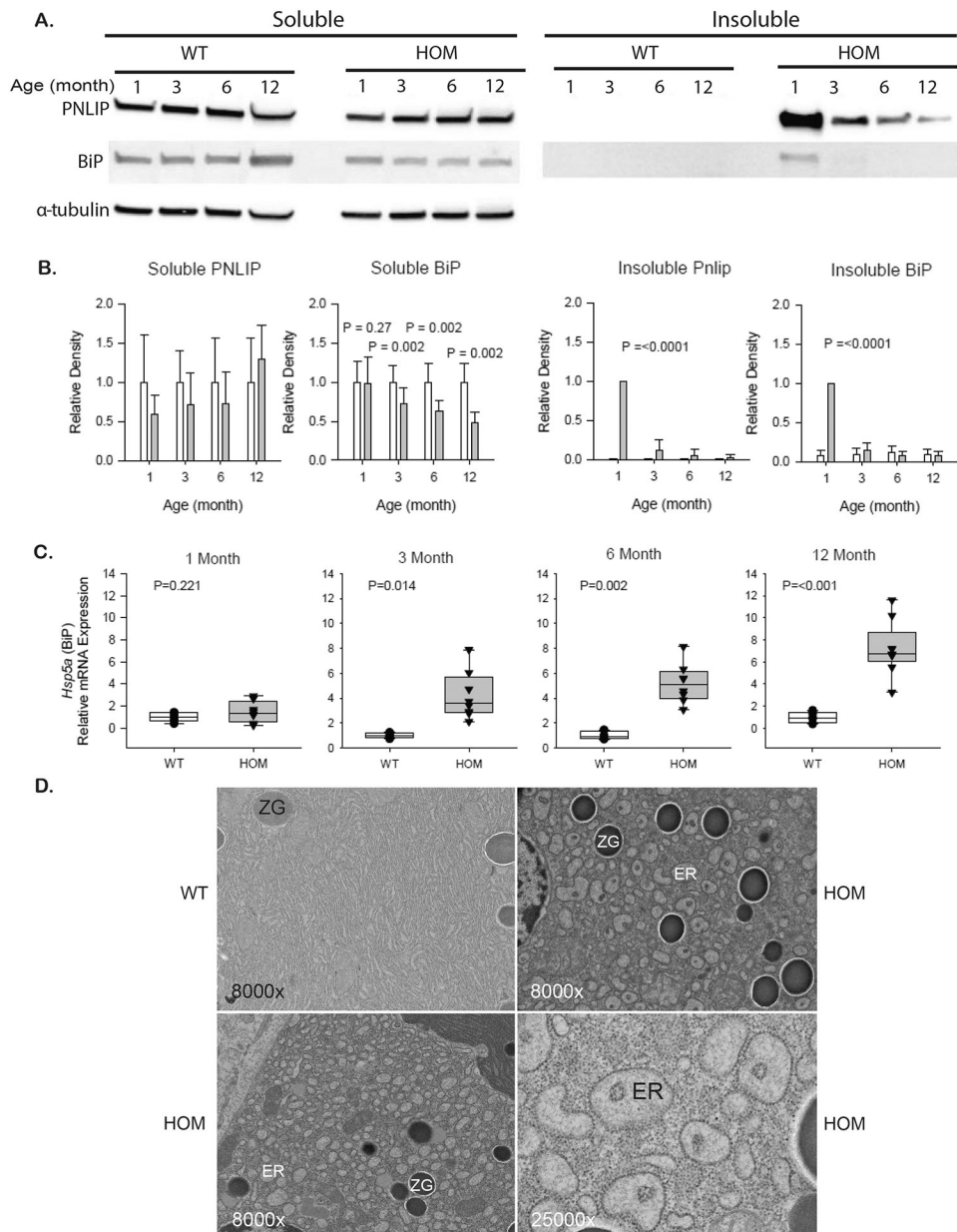


Fig 7. PNLIP misfolding and ER stress in the pancreas of *Pnlip* p.T221M homozygous (HOM) and wild type (WT) mice with age. **A.** Representative immunoblots of PNLIP and BiP in the detergent-soluble and -insoluble fractions of pancreatic protein extracts, and α -tubulin served as an endogenous control for the soluble fractions. **B.** The quantification graphs of immunoblot analysis of PNLIP and BiP in **A.** **C.** qPCR analysis of *Hsp5a* (BiP) mRNA abundance in the mouse pancreatic RNA extracts, and Rpl13a served as a control. The results are expressed as fold change relative to the mean of the results of age-matched WT mice. **D.** Representative of transmission electron micrographs (TEM) of the mouse pancreatic sections at 6 months shows a profound dilation of the ER in the HOM pancreas

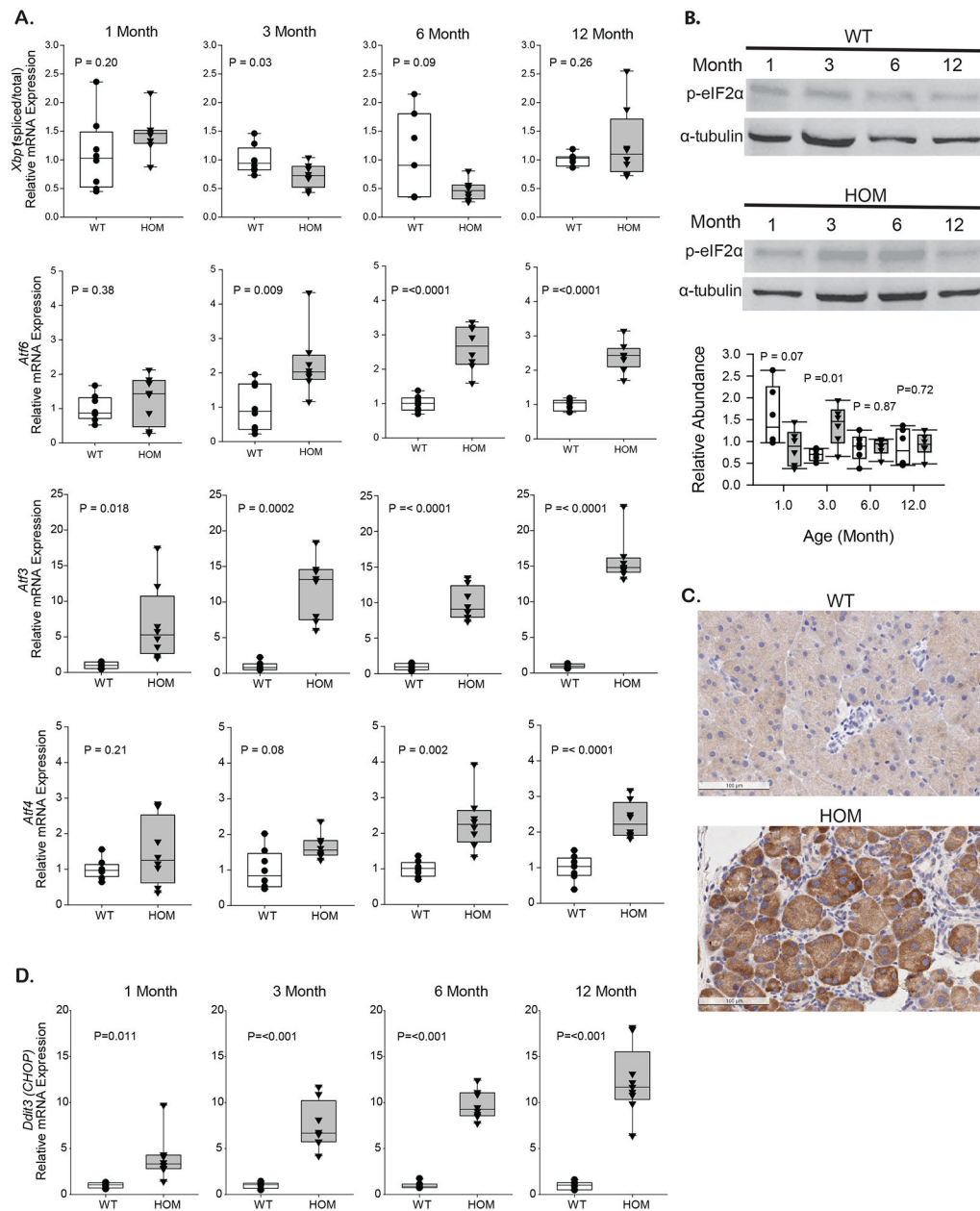
(8000x and 25000x). ER: endoplasmic reticulum; ZG: zymogen granule. n = 6 per genotype per age point in *A, B, C*; n = 3 in *D*.

Author Manuscript

Author Manuscript

Author Manuscript

Author Manuscript

**Fig 8.**

Age-dependent activation of the unfolded protein response (UPR) in the pancreas of *Pnlip* T221M homozygous (HOM) and wild type (WT) mice. **A.** qPCR analysis of mRNA abundance of various markers of the UPR in the mouse pancreatic RNA extracts, and Rpl13a served as controls. The markers include *Xbp1* mRNA splicing, *Atf6*, *Atf4*, and *Atf3*. **B.** Representative immunoblots of phosphorylated eIF2 α (p-eIF2 α) in the detergent-soluble pancreatic protein extracts, and α -tubulin served as an endogenous control (top panel); the quantification graph of immunoblot analysis of p-eIF2 α (bottom panel). **C.** Immunohistochemistry of the mouse pancreatic sections for p-eIF2 α . **D.** qPCR analysis of mRNA abundance of *Ddit3* (CHOP) in the mouse pancreatic RNA extracts, and Rpl13a served as controls. n = 6 per genotype per age point except for n = 3 in **C**.

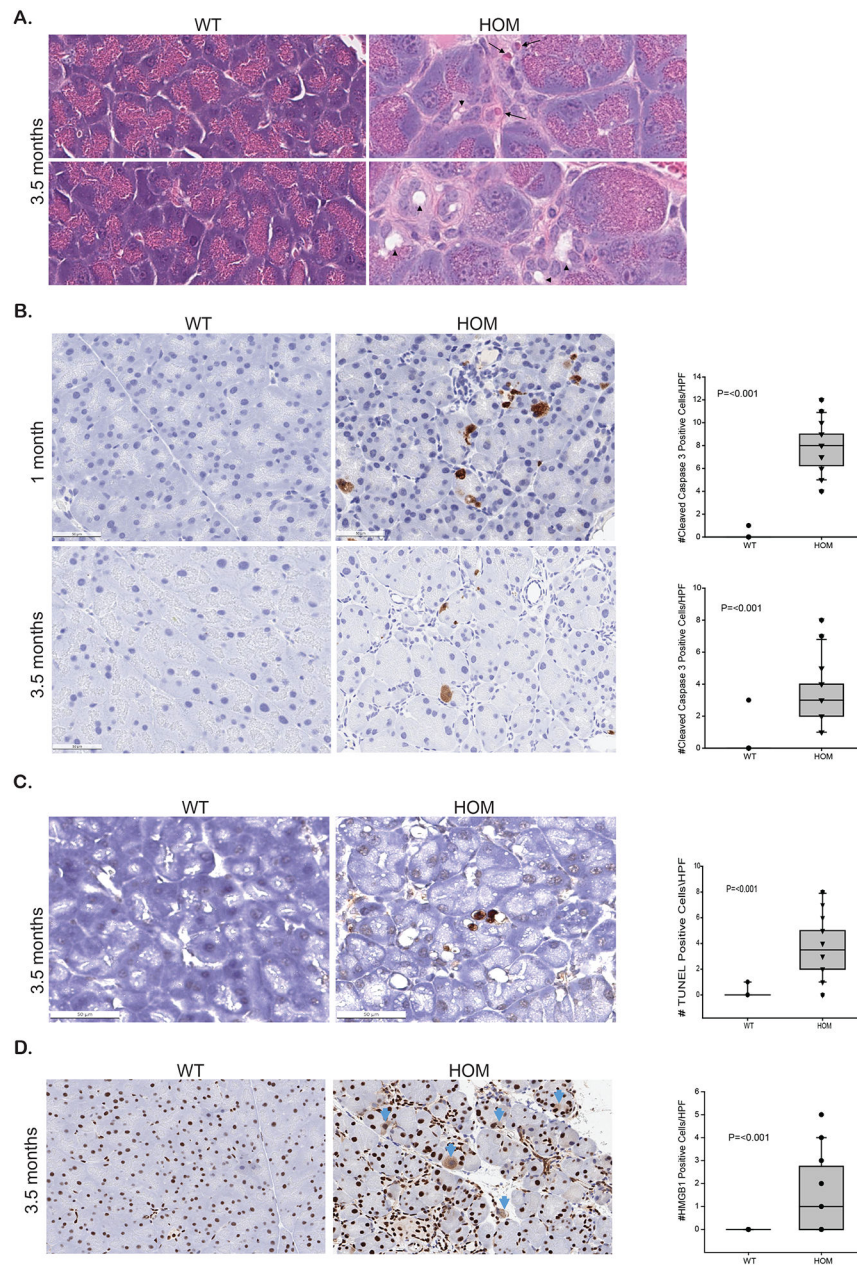


Fig 9. Increased cell death in the pancreas of *Pnlip* p.T221M homozygous (HOM) and wild type (WT) mice at age 3.5 months. **A.** H&E staining (40 x magnification) of the pancreatic sections showing both necrotic (arrow head) and apoptotic (long arrow) cells and larger acinar cells. **B.** Immunohistochemistry staining of cleaved-caspase 3 in the pancreatic sections (brown), and the staining on the pancreatic sections at 1 month also included. **C.** TUNEL staining of the pancreatic sections (brown). **D.** Immunohistochemistry staining of high mobility group box 1 (HMGB1) in the pancreatic section showing increased nuclear to cytoplasmic HMGB1 transition (arrowhead). In *B-D*, the corresponding quantification graph is listed on the right. $n=3$ in *A* and $n=10$ in *B-D*.